Supplementary Material to the article

"Probing of the superconducting order parameter in weakly underdoped $BaFe_{1.92}Ni_{0.08}As_2$ by two complementary techniques"

Section I. Sample characterization. Figure S1 shows the superconducting transition of the studied single crystal obtained in resistive and magnetic probes. The bulk critical temperature is about $T_c \approx 18\,\mathrm{K}$, with the transition width $\Delta T_c \approx 1.1\,\mathrm{K}$ and $\Delta T_c \approx 1.2\,\mathrm{K}$, as determined by $R(T)$ and $\chi(T)$ measurements, respectively. The decreasing $R(T)$ trend above T_c is typical for underdoped BFNA compounds (see, for example, Fig. 4.2a in [1]).

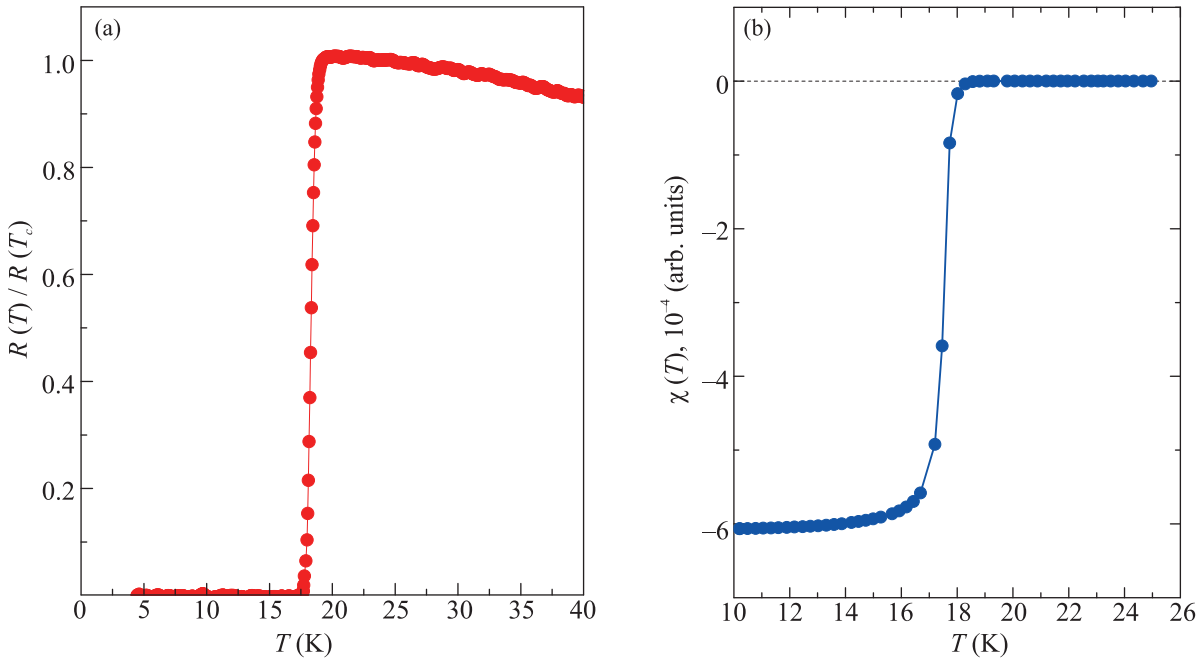

Fig. S1. Temperature dependence of resistance (left panel, the same curve as shown in Fig. 4 by gray circles) and magnetic susceptibility (right panel) of the studied $BaFe_{1.92}Ni_{0.08}As_2$ single crystal

Section II. Andreev spectroscopy of planar break-junctions: experimental details.

a. On the modeling of the planar break-junctions. The supposed scheme of the break-junction geometry is presented by us earlier, see Fig. 1 in [2]. After a cryogenic cleavage of a platelet single crystal (oriented along the *ab*-planes), two cryogenic surfaces with steps and terraces onto them are typically formed. Under gentle mechanical tuning of the holder curvature, the cryogenic surfaces slide along the *ab*-planes, touching via terraces and thus forming a planar superconductor–barrier–superconductor junction.

Since impossibility of direct experimental check of the contact geometry and interior, one could consider any appropriate model that is able to qualitatively describe the incoherent Andreev transport observed in our experiment and the absence of the supercurrent. Likely, we concern the obtained structure as SnInS (S – superconductor, I – insulator, n – thin normal

metal), with equivalent S banks. The cryogenic surfaces (with superconducting properties degraded under destruction) could act as n-layer, rather than actual gap between the S-banks. Formally, as required by the theory, in order to experimentally observe incoherent MAR effect, the insulator with rather high transparency ($Z < 0.5$) and the areas, which metallic properties are concerned not only as the gapless population of the electron density of states, but in principal high possibility generation of electron-hole excitation.

b. On the alternative interpretations of the $dI(V)/dV$ features. Although interference $dI(V)/dV$ features at $|eV| = (\Delta_L + \Delta_S)$ in single crystals of two-gap superconductors were not detected in the experiment unambiguously so far, one may suppose such interpretation to the dip labeled in Fig. 1b as $n_L^{\text{out}} = 2$, since at $T \ll T_c$ its position is close to $(\Delta_L^{\text{in}} + \Delta_S)$. In this case, due to more rapid decreasing of $\Delta_S(T)$ in the vicinity of T_c, the position of this dip would also shift to zero more rapidly at high temperatures, as compared to $\Delta_L(T)$. Contrary, the position of the considered dip $n_L^{\text{out}} = 2$ remains almost two times lower than that of the fundamental harmonic $n_L^{\text{out}} = 1$ within all the temperature range (see open circles in the lower panel of Fig. 2, the main text), thus replicating the temperature trend $\Delta_L(T)$. Therefore, we interpret this dip as the second subharmonic of Δ_L^{out}.

Section III. On the choosing of the H_{c1} criterion. The used experimental technique of the magnetization curve measurements by using Hall probe has a set of advantages and disadvantages. The number of experimental points per $M(H)$ curve drastically rises (for example, as compared to SQUID magnetometer measurements), but the probing is located only in the area of the sample, that corresponds to the geometric dimensions of the Hall probe. In this area, likely is the presence of minor inhomogeneities of the superconducting phase, those almost undetectable in integral probing by VSM or SQUID, and affecting the beginning of $M(H)$ deviation from Meissner trend. Therefore, we choose the criterion higher than the level of noise (and therefore excluding parasitic contributions of the sample inhomogeneities), as the basic one in order to determine H_{c1}.

As an example, three various criteria A, B, and C are shown (horizontal lines exceeding the noise level in $sqrt(M)$ on H dependences). The corresponding $H_{c1}(T)$ curves obtained using these criteria (as the crossing between experimental data and the corresponding horizontal line) and their fits with two-band α-model are presented in (b) panel of Fig. S2. The normalized $H_{c1}(T)/H_{c1}(0)$ curves obtained using various criteria are compared in (c) panel. Despite substantial variation of the absolute H_{c1} values, the temperature trend $H_{c1}(T)/H_{c1}(0)$ remains almost the same, as shown in Fig. S2c.

In the lower panel of Fig. S2c, we show the scaling quality as a relative deviation between the $H_{c1}^B(T)$ curve obtained using criterion B (taking as a basis; this data is shown in Fig. 4 in the main text of the paper) and other $H_{c1}i(T)$ curves. The deviation is taken as $[H_{c1}^A - H_{c1}i]/H_{c1}^B(0)$. Obviously, the deviation does not exceed $\pm 2.5\,\%$ H_{c1}^B within the whole temperature range.

In the Table S1 below, we summarize the superconducting parameters determined from the best fits of $H_{c1}(T)$ curves corresponding to A, B, and C criteria. For all the criteria, we take the values $\Delta_S^{\text{out}} = 1.6\,\text{meV}$, $\Delta_L^{\text{in}} = 3.2\,\text{meV}$, and $\Delta_L^{\text{out}} = 4.5\,\text{meV}$ from IMARE experiment, whereas the weight coefficient of the Δ_S bands contribution ϕ and the Δ_S anisotropy A_S of were fitting parameters. The ϕ range varies within $\pm 5\,\%\,\phi$, whereas the A_S value spread is about $\pm 12\,\%$ of

the average $A_S \approx 55\,\%$. Therefore, the choice of the criterion does not change substantially the characteristic ratios of the superconducting gaps determining from the fit.

Table S1. Fitting parameters for various H_{c1} criteria: the low-temperature value $H_{c1}(0)$, the weigth contribution of the bands with the small gap φ, and Δ_S anisotropy A_S

Criterion	$H_{c1}(0)$	ϕ	A_S	
A	171.3	0.597	0.64	
B	**146.8**	**0.619**	**0.56**	← This criterion was taken in the main text of the paper.
C	122.8	0.66	0.43	

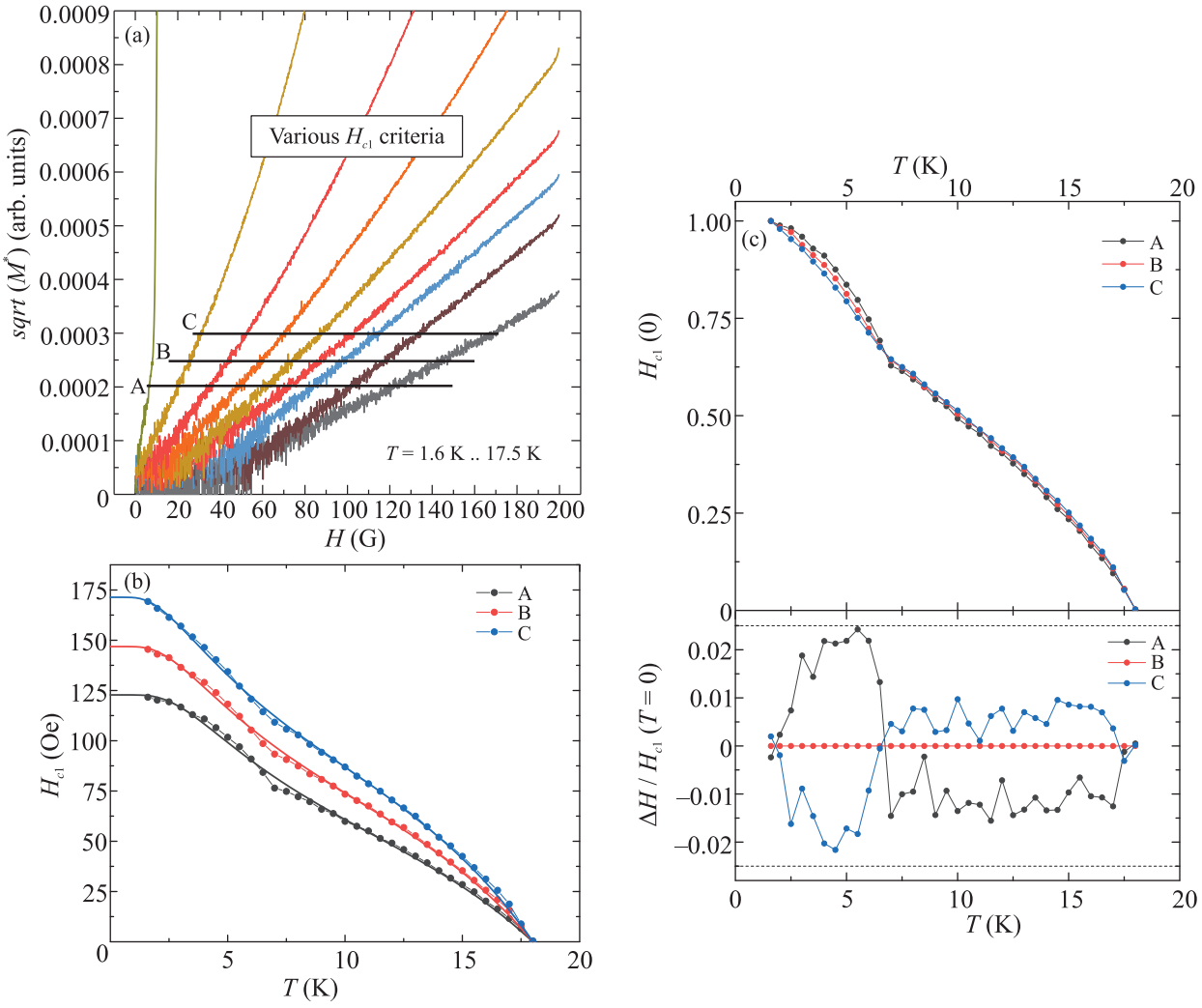

Fig. S2. (a) – Various criteria exceeding the noise level of $sqrt(M(H))$ curves. (b) – The $H_{c1}(T)$ dependences obtained using A, B, and C criteria with two-band α-model fits (with anisotropic small gap). (c) – Scaling of the $H_{c1}(T)$ dependences obtained using various criteria. In the lower panel, the deviation of the curves in relation to $H_{c1}(0)$ dependence obtained using criterion B is shown

1. X. Lu, *Phase Diagram and Magnetic Excitations of $BaFe_{2-x}Ni_xAs_2$: A Neutron Scattering Study*, Springer Theses, Springer, Singapore (2017); DOI:10.1007/978-981-10-4998-9.
2. Z. Popovic, S. A. Kuzmichev, and T. E. Kuzmicheva, J. Appl. Phys. **128**, 013901 (2020).